Allosteric Intermediates in Hemoglobin. 1. Nanosecond Time-Resolved Circular Dichroism Spectroscopy†

Sofie C. Björling,‡ Robert A. Goldbeck,* Sarah J. Paquette, Steven J. Milder,§ and David S. Kliger

Department of Chemistry and Biochemistry, University of California at Santa Cruz, Santa Cruz, California 95064

Received September 19, 1995; Revised Manuscript Received February 27, 1996⊗

ABSTRACT: Time-resolved circular dichroism (TRCD) studies performed on photolyzed hemoglobin−CO complex (HbCO) probe room temperature protein relaxations in Hb, including the R → T allosteric transition. TRCD spectroscopy of photolysis intermediates in the near-UV (250−400 nm) spectral region provides a diagnostic for T-like structure at the $\alpha_1\beta_2$ interface via the effect of quaternary structure on the UV CD of aromatic residues. The TRCD of porphyrin-based transitions in the UV and Soret regions, reflecting transition-dipole couplings between hemes and aromatic residues over a radius wide enough to permit heme-interface and inter-dimer interactions, is modulated by the tertiary and quaternary structure of photolysis intermediates. In the allosteric core model of Hb cooperativity, Fe−CO bond breakage initiates a heme structural change, thought to be heme doming, that is transmitted to the $\alpha_1\beta_2$ interface via the F helix. The TRCD results, analyzed in light of kinetic information from time-resolved absorption studies, suggest specific features for the mechanism by which the ensuing tertiary and quaternary conformational changes propagate through the protein. In particular, the UV-TRCD indicates that the $\alpha_1\beta_2$ interface responds within several hundred nanoseconds to initial events at the heme by shifting from an R toward a T-like interface. The appearance of T-like character at the $\alpha_1\beta_2$ interface tens of microseconds before the appearance of equilibrated T state deoxyHb indicates that the R → T transition in photolyzed HbCO is a stepwise process, as previously suggested by time-resolved resonance Raman studies.

The molecular basis for the cooperative binding of ligands to hemoglobin (Hb)[1] remains incompletely understood, although hemoglobin was the first allosteric protein whose structure was determined by X-ray crystallography (Perutz et al., 1960). Much attention has since been focused on the mechanism by which the oxygen affinity of Hb increases with increasing oxygen saturation, a property that greatly increases the efficiency of O_2 transfer from the lungs to the tissues. Hb cooperativitiy is mediated by a ligation-dependent equilibrium between structures of differing ligand-binding affinities. The high-affinity oxy, or R (relaxed), and low-affinity deoxy, or T (tense), forms differ both in quaternary structure, i.e., the relative arrangements of the four subunits, and in tertiary structure, the conformation of the individual subunits. The quaternary structural change associated with the R → T transition involves a relative motion between the two $\alpha\beta$ dimers making up the tetramer that corresponds to a rotation by 15° and a translation by 0.8 Å, the two structures being stabilized by different arrangements of inter-dimer hydrogen bonds and salt bridges. It is not firmly established, however, just how the change in stereochemistry at and around the heme caused by the reaction of heme iron with O_2 and other ligands affects the interfacial forces to trigger interconversion of the T and R forms (Perutz, 1970, 1972, 1979; Perutz et al., 1987).

Many time-resolved absorption studies have examined the photolysis of the hemoglobin carbonyl adduct (HbCO) in order to better understand the mechanism of cooperative ligand binding (Hofrichter et al., 1983, 1985; Murray et al., 1988; Jones et al., 1992). To this end, knowledge of the equilibrium R and T structures of Hb and the thermodynamics of their interconversion does not present a complete picture of cooperativity without an understanding of the rates of interconversion, i.e., a kinetic mechanism. This mechanism appears to be complex in hemoglobin. Kinetic ligand-photodissociation studies find several transition states linked by intermediates that correspond to a series of conformational changes in the protein culminating in the quaternary structure change associated with cooperativity. Elucidation of these kinetic steps from their spectral signatures during HbCO photolysis can reveal the dynamics of the mechanism by which the protein subunits communicate their ligation information to one another during allosteric switching between equilibrium quaternary conformations.

The picture of HbCO photolysis emerging from the great number of structural and kinetic studies that have been performed on Hb forms a background to the present work briefly summarized as follows. The initial reactant is the ground electronic state of HbCO, containing a diamagnetic iron atom lying in the heme plane that is axially coordinated by CO and an imidazole nitrogen from the proximal histidine

† Financial support for this work was provided by the National Institutes of Health, Grant GM-35158.

* Author to whom correspondence should be addressed.

‡ Present address: Department of Medical Biophysics, MBB, Karolinska Institute, S-171 77 Stockholm, Sweden.

§ Deceased December 23, 1993.

⊗ Abstract published in *Advance ACS Abstracts,* June 15, 1996.

[1] Abbreviations: CD, circular dichroism; ΔCD, CD of photolyzed sample minus CD of pre-photolysis sample; ΔOD, optical density of photolyzed sample minus optical density of pre-photolysis sample; fs, femtosecond; Hb, human hemoglobin A; LEP, left elliptically polarized; Mb, myoglobin; Nd:YAG, neodymium yttrium aluminum garnet; nm, nanometer; NMR, nuclear magnetic resonance; ns, nanosecond; OD, optical density; OMA, optical multichannel analyzer; $\pi\pi^*$, π-bonding to π-antibonding orbital excitation; REP, right elliptically polarized; TRCD, time-resolved circular dichroism; TROD, time-resolved optical density; UV, ultraviolet.

S0006-2960(95)02247-1 CCC: $12.00

residue. Karplus and co-workers (Gelin & Karplus, 1977; Gelin et al., 1983) have pointed out that the geometry of the Fe−histidine bond, which is perpendicular to the heme plane in HbCO and 10° tilted in deoxyHb (Baldwin & Chothea, 1979), may play an important role in cooperative ligand binding in Hb. Accordingly, elucidation of the coupling between aspects of heme stereochemistry such as the Fe−histidine bond angle and relaxations in protein tertiary and quaternary structure following ligand photodissociation is a major focus of time-resolved spectral studies. The initial event in these studies, photodissociation of the heme Fe−CO bond, is extremly rapid, occurring in less than 50 fs in hemoglobin, myoglobin, and protoheme (Petrich et al., 1988). Electronically excited, unligated heme decays to its ground state with a lifetime of 300 fs (Petrich et al., 1988). Geminate recombination (prompt rebinding of photolyzed ligand to the same heme from which it dissociated) occurs with a yield of about 40% (Hofrichter et al., 1983; Murray et al., 1988) and an approximate lifetime of 20 ns (Jones et al., 1992). The ligand-dissociative excited state has been assigned from semiempirical calculations (Waleh & Loew, 1982) as a low-lying triplet ligand field state, Hb($^3T_1$). Relaxation of electronic excitation gives a ground state of spin $S = 2$, Hb†($^5T_1$), that has not yet fully relaxed to the equilibrium tertiary structure of deoxyHb, Hb($^5T_1$). The increased Fe atomic radius accompanying the paramagnetic spin states of both the dissociative and the product electronic states suggests that some doming of the heme appears promptly, i.e., subpicosecond, as also thought to occur in myglobin (Jackson et al., 1994). However, this prompt doming may not completely accommodate the forces (Fe atomic size and imidazole hydrogen and pyrrole nitrogen repulsions) driving the iron out of the heme plane, and it has been suggested that much of the unrelaxed character of Hb†($^5T_1$) may arise from an impediment to complete doming imposed on local tertiary structure near the heme by the quaternary structure of the protein in its R state (Petrich et al., 1987, 1988). The dynamical coupling between quaternary and tertiary structure involved in Hb cooperativity is thus expected to produce more complex relaxation behavior than observed in Mb, although relaxation of iron-out-of-plane motion is observed in band III (763 nm) to be highly nonexponential over picosecond to microsecond time scales in Mb, suggestive of a strong coupling between iron−porphyrin motion and tertiary structure remote from the heme (Jackson et al., 1994). In hemoglobin, evidence from time-resolved resonance Raman suggests that the final stage in heme doming occurs with a time constant of about 100 ns (Spiro et al., 1990). The tertiary protein relaxation accommodating full out-of-heme-plane displacement of the iron may also be accompanied by the initial tilt of the proximal histidine−Fe bond leading toward the fully-tilted deoxy state. In the allosteric core model of Gelin and Karplus (1977), a change in histidine−heme geometry is transmitted to the $\alpha_1\beta_2$ interface via the F helix conduit. The resulting change in forces acting at the interface allows the inter-subunit interactions to find a new free energy minimum corresponding to the T quaternary state. Accordingly, a change in the optical absorption and resonance Raman properties of the hemes with a time constant of 20−30 μs, assigned to relaxation of subunit tertiary structure near the hemes, is thought to signal completion of the R → T quaternary structure change (Friedman, 1985; Findsen et al., 1985). The time-resolved resonance Raman spectral changes in particular are indicative of full accommodation of the histidine tilt to its equilibrium position in T state deoxy heme. Two longer relaxation times seen in time-resolved absorption studies of HbCO photolysis, ca. 0.2 and 3 ms at 1 mM dissolved CO, are dependent on CO concentration and are attributed to second-order rebinding of CO to R and T state hemoglobin, respectively (Hofrichter et al., 1983).

The principal question addressed by the present work is does the initial rearrangement at the $\alpha_1\beta_2$ interface trigger a concerted R → T transition or, as can reasonably be expected for a structure as complex as that of Hb, does a change in subunit tertiary structure propagate in a stepwise manner toward the final quaternary structure? Previous evidence for a stepwise R → T transition comes from time-resolved resonance Raman studies that find sub-microsecond changes in aromatic residues at the dimer interfaces (Rodgers et al., 1992; Jayaraman et al., 1995) and from time-resolved absorption spectroscopy of the heme chromophore (Hofrichter et al., 1985; Goldbeck et al., 1996).

In this study we investigate the recombination of Hb with CO after photolysis of HbCO using time-resolved circular dichroism (TRCD) spectroscopy in the nanosecond to millisecond time regime. We discuss the results of this qualitative kinetic study in the context of the quantitative kinetic analysis of unpolarized time-resolved absorption spectra, obtained under similar conditions (high photolysis, high CO saturation), presented in the following paper in this issue (Goldbeck et al., 1996). Previous nanosecond (ns) CD work on HbCO (Lewis et al., 1985; Einterz et al., 1985) served mainly to demonstrate the ellipsometric CD method used here and presented data at only a limited number of wavelengths. The present work is the first ns multichannel spectral study of TRCD in hemoglobin and is also the first TRCD study to probe the CD of kinetic intermediates in a hemeprotein over a spectral range that includes contributions from aromatic residues as well as from heme-based transitions. In doing so, it was anticipated that the near-UV (250−400 nm) and Soret (400−460 nm) regions would show distinct and complementary CD sensitivities to conformational changes. The increased sensitivity of CD spectroscopy in general to molecular conformation is a principle well established from static CD measurements. The ability of fast CD spectroscopy in particular to provide structural information about phototransformations in biomolecules was recently demonstrated in studies of the photoregulatory plant pigment phytochrome (Björling et al., 1992; Chen et al., 1993). The UV-CD spectral attributes that characterize the equilibrium structures of liganded and deliganded Hb have been studied by Perutz and co-workers (1974a). Most significant for the principal question addressed in the present work concerning the stepwise nature of the allosteric transition in Hb is the assignment of a negative peak in the aromatic region near 287 nm as a characteristic of the T quaternary structure. The observation of sub-microsecond changes in the aromatic CD presented below is thus found to be strong evidence for the existence of an initial step in the non-concerted transformation of R to T.

MATERIALS AND METHODS

Human hemoglobin was prepared from fresh blood using the method of Geraci et al. (1969). Each sample was

prepared by deoxygenating 40 mL of pH 7.3, 0.1 M sodium phosphate buffer with Ar for at least $^1/_2$ h before the addition of hemoglobin droplets. The concentration of Hb samples was approximately 120 μM in heme. Hemoglobin solutions were vacuum filtered and saturated with CO for 1−2 h (argon for deoxyHb) in a home-made air-tight cell. Sodium dithionite (Sigma) was added to Hb samples to remove any traces of oxygen. Stock solutions of $Na_2S_2O_4$ were prepared by dissolving crystals in deoxygenated buffer, and aliquots of this stock were added to Hb samples to yield a final dithionite concentration of 540 μM. Sample cells with pathlengths of 2 and 0.5 mm were used in the UV and Soret, respectively, permitting use of the same Hb and $Na_2S_2O_4$ concentrations for the two spectral regions.

The samples were photolyzed by 7-ns, 532-nm light pulses from a Nd:YAG laser. Laser energies of 12−15 mJ/pulse and beam diameters of 3−7 mm were used. Xenon flashlamps producing 5-μs pulses were used as probe sources. The probe light was dispersed with a spectrograph using a 150 groove/mm grating and input slit width of 250 μm. When we were working in the Soret spectral region, a filter (O-52, Corning) that was opaque below 360 nm was used in front of the spectrograph to avoid detection of light diffracted by the grating in second order.

Time-resolved measurements were made with a time-gated optical multichannel analyzer (OMA) detection system (PAR 1420 detector). The time gate of the OMA was varied in width between 150 ns and 5 μs. The shortest gate width was used for the 300-ns delay time in the Soret spectral region, with the gate in this case opening 300 ns and closing 450 ns after the laser photolysis pulse. Other gate widths used in the Soret were 1 and 4 μs for the 1−15- and 50−500-μs delay times, respectively. Gate widths in the UV were 1 and 5 μs for the 0.5−15- and 50−500-μs delays, respectively. The gate and flashlamp pulses were delayed jointly relative to the laser over a time span ranging from nanoseconds to milliseconds. Data at each delay time was obtained in ten sets of 128 averages. Measurements for the various probe times were taken in pseudo-random order to minimize the introduction of systematic errors in the apparent kinetics from small variations in experimental conditions (e.g., sample integrity, temperature) during data collection.

All spectra were obtained on the ns ellipsometric TRCD apparatus developed in this laboratory. The ellipsometric TRCD technique is described in detail elsewhere (Lewis et al., 1985; Goldbeck & Kliger, 1993, and references therein). Briefly, elliptically polarized light is produced by introducing a strained (1° retardance) fused-silica plate in the path of a linearly polarized probe beam. The strain axis is set at +45° or −45° relative to the polarization axis of the incident light, producing right elliptically (REP) or left elliptically (LEP) polarized light, respectively. A circularly dichroic sample affects the relative ellipticities of REP and LEP. The change in ellipticity is determined from the difference between absolute intensity measurements for REP and LEP taken along the direction of the minor elliptical axis, accomplished by passing the light through a second polarizer oriented perpendicularly to the original polarization axis. The CD signal is calculated as

$$S = (I_R - I_L)/(I_R + I_L) \quad (1)$$

where I_R and I_L are the detected intensities when REP or LEP is incident on the sample. The signal is related to the circular dichroism, $\Delta\epsilon$, by

$$\Delta\epsilon = S\delta/Cz \quad (2)$$

where δ is the retardation of the strain plate in radians, C is the sample concentration in mol/L, and z is the path length in cm. The CD data presented here was smoothed according to the least-squares procedure of Savitzky and Golay (1964) using 9 or 17 points (0.6 nm/point) to yield the optimal smoothing consistent with the spectral resolution. CD spectra were limited to 250 nm by the optical properties of the calcite polarizers.

The transient difference CD signals ($\Delta\Delta\epsilon$) are computed as the CD measured at the specific delay time after photolysis minus the CD of unphotolyzed HbCO. Corresponding transient difference OD spectra (ΔOD) are calculated using the I_R and I_L intensities from the TRCD measurements according to

$$\Delta OD = -\log_{10}[(I_R + I_L)_t/(I_R + I_L)_{t=0}] \quad (3)$$

where the numerator is the average of REP and LEP light intensities for the intermediate probed at time t, and the denominator is the corresponding average of intensities for the unphotolyzed sample. We point out that this is not a rigorous calculation of the difference OD spectrum because of small second-order contributions to $I_R + I_L$ from anisotropic absorption and birefringence properties of the sample (Björling et al., 1991). However, it was found to suffice in the present study as a means for verifying the formation of species of interest through comparison with accurate difference OD spectra presented in the accompanying paper.

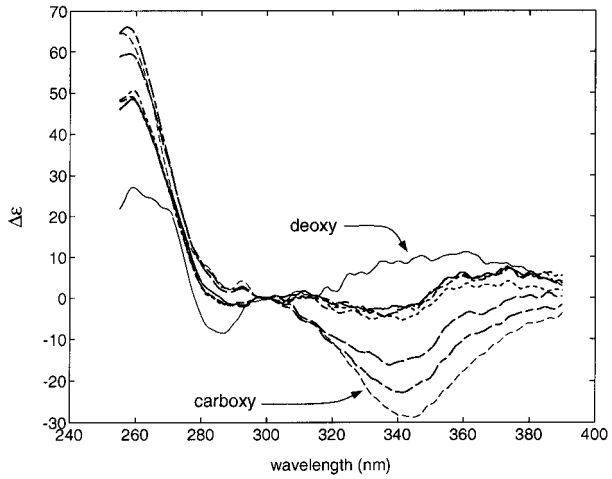

FIGURE 1: UV TRCD spectra measured at 500 ns (—), 5 μs (- - -), 10 μs (···), 15 μs (-·-), 50 μs (— — —), and 500 μs (— - —) after photodissociation of HbCO (heavy lines) and equilibrium UV CD spectra of Hb (—) and HbCO (- - -) measured on the TRCD apparatus (light lines).

RESULTS

Near-UV Spectral Region. Figure 1 shows absolute CD spectra measured in the 250−400-nm UV spectral region for unphotolyzed HbCO and equilibrium deoxyHb, as well as time-resolved spectra measured at six delay times, 0.5, 5, 10, 15, 50, and 500 μs, after HbCO photolysis. The CD spectra shown are base line corrected to give identical $\Delta\epsilon$ values near 305 and 410 nm, isosbestics of the static HbCO and deoxyHb CD spectra. The HbCO and deoxyHb spectra

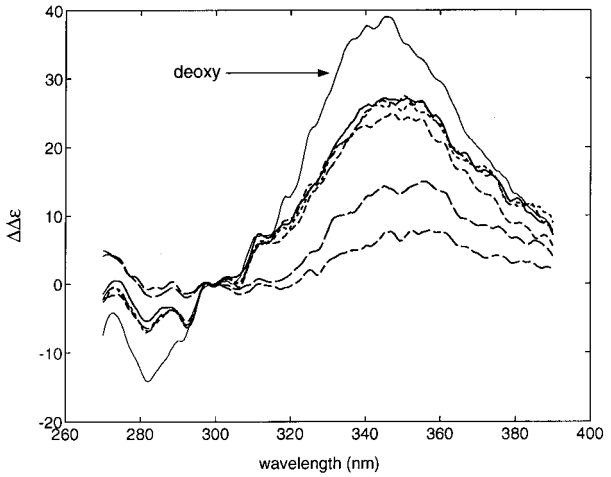

FIGURE 2: Photolysis difference CD spectra for the data in Figure 1: 500 ns (—), 5 μs (- - -), 10 μs (•••), 15 μs (-•-), 50 μs (— — —), and 500 μs (— - —) after photodissociation (heavy lines) and static Hb spectrum (—) (light line).

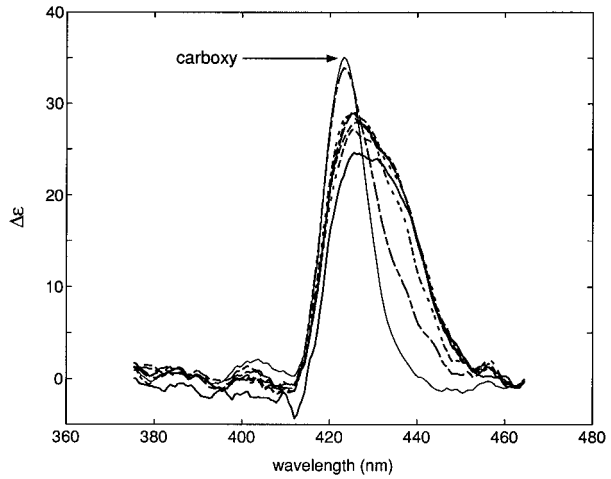

FIGURE 3: Soret region TRCD spectra measured at 300 ns (—), 1 μs (— —), 5 μs (- - -), 10 μs (•••), 15 μs (-•-), 50 μs (— — —), and 500 μs (— - —) after photodissociation of HbCO (heavy lines) and CD spectrum of HbCO (—) (light line).

obtained in this way correspond well with steady-state CD spectra measured on a conventional CD spectrometer. The largest differences between the absolute TRCD spectra measured at 50 and 500 μs are an increase in the positive CD band and a growing in of negative ellipticity around 350 nm. Both of these bands are assigned to porphyrin-based $\pi\pi^*$ transitions, the former corresponding to the L band in porphyrin and the latter to the N band. The large increase in CD in the region near 260 nm accompanying ligation is attributed to structural changes at the heme, as is the increase in negative ellipticity near 350 nm (Perutz et al., 1974a). The changes between 50 and 500 μs are thus consistent with the rebinding of CO to the protein in its R state between these probe times, as expected from previous studies of Hb rebinding kinetics (Hofrichter et al., 1983, 1985; Murray et al., 1988).

Because of incomplete photolysis (photolysis yield about 90%) and geminate recombination (effective yield about 30%), the absolute TRCD spectra presented here are mixtures of time-evolving signals from the transient species of interest and a constant contribution from unphotolyzed and promptly recombined HbCO. It is therefore useful to compute difference CD signals in order to remove the constant CD background signal (see Materials and Methods). Figure 2 shows the ΔCD spectra (time-resolved spectra of photolyzed HbCO minus unphotolyzed HbCO spectrum) calculated from the CD data shown in Figure 1. The CD changes in the aromatic spectral region near 285 nm are of particular interest. Note that a prominent negative CD change appears at this wavelength after photolysis that is almost as fully developed at the earliest time probed, 500 ns, as it is at 5−15 μs. Given that this signal is averaged over the 1-μs duration of the OMA gate, the appearance of a signal that is roughly 80% complete suggests that the first-order time constant for the rate process leading to the negative ellipticity absorber is approximately 500 ns. As discussed further below, this CD change corresponds to the appearance of a negative CD band characteristic of T quaternary structure (Perutz et al., 1974a). Although the fast time constant inferred from the rise of the aromatic TRCD is rather uncertain, being at the edge of the instrument time resolution, we point out that a 500-ns time constnat is also in good agreement with the 430-ns time constant observed in a time-resolved optical rotatory dispersion (TRORD) study of HbCO in the Soret region by Shapiro et al. (1995). This TRORD study demonstrated the enhanced sensitivity of kinetic ORD and CD spectroscopy in the Soret region to structural relaxations associated with the R → T transition. The time evolution of the 350-nm ΔCD band, on the other hand, appears to be a simple monotonic decay (the small increase in intensity between 10 and 15 μs is presumably artifactual), but the ΔCD signal decays more quickly at long times, 50−500 μs, than does the ΔOD of this band (see accompanying paper, Figure 2b). A parallel increase in the decay of ΔCD intensity is also found for the Soret region (see below).

Soret Spectral Region. Figure 3 shows the CD spectrum of HbCO measured on the TRCD apparatus in the Soret spectral region, and seven TRCD spectra obtained at different probe times after HbCO photolysis (0.3, 1, 5, 10, 15, 50, and 500 μs). The spectra have been adjusted with offsets to give similar $\Delta\epsilon$ values around 390 and 480 nm, as these are found from static spectra to be isodichroic points for HbCO and deoxyHb. There is a red shift of the Soret CD band and an increase of its rotational strength upon deligation, as is seen when comparing the spectra for HbCO and deoxyHb. The earliest probe time shows characteristics of a deoxy heme-like spectrum, with a red shift of the CD maximum and slightly negative ellipticity around 400 nm. The later probe times exhibit spectra increasingly similar to the parent HbCO species.

Figure 4 shows the ΔCD calculated from the data shown in Figure 3. The divergence between the time evolution observed for ΔCD and that found for the ΔOD is of particular interest. The earliest TRCD measurements begin at 300 ns, well after geminate recombination is complete and rotational diffusion (time constant approximately 30 ns) has eliminated any photoselection-induced orientation effects in the spectral measurements. The evolution observed in the ΔOD spectra starting at this time and extending to 15 μs, a subset of the data shown in Figure 2a of the accompanying paper, corresponds to a 13% decrease in the magnitude of the bleaching trough near 415 nm and a 4% decrease of the peak at 433 nm. This is expected as diffusive recombination of CO, the dominant mechanism for ΔOD evolution, proceeds slowly on this time scale, although some changes are also due to the R − T difference spectrum. The Soret band of

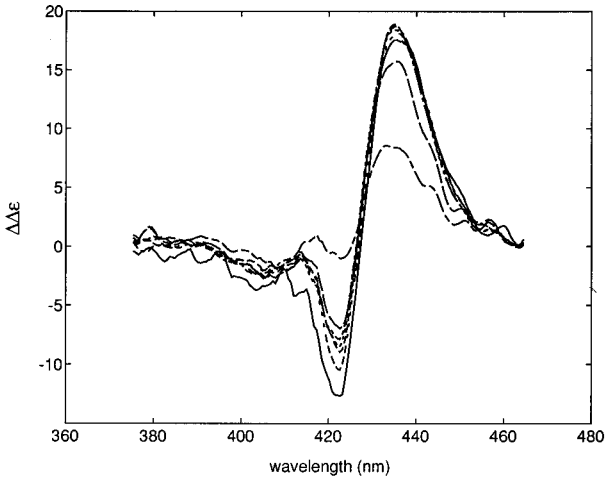

FIGURE 4: Photolysis difference CD spectra for the data in Figure 3: 300 ns (—), 1 μs (— —), 5 μs (- - -), 10 μs (•••), 15 μs (-•-), 50 μs (— — —) and 500 μs (— - —) after photodissociation.

the T form is slightly blue shifted and is 20% higher in intensity than R (Perutz et al., 1974a). The ΔCD spectra, however, show larger and more complex changes over the same time span. This is most obvious for the CD trough near 420 nm in Figure 4, which decreases in magnitude by 40% over the 0.3−15-μs time interval. This positive-going trend also appears in the ΔCD peak near 435 nm, which increases in intensity by 7% between 0.3 and 15 μs despite a decrease in the corresponding ΔOD. The overall result is an increase in the observed asymmetry of the ΔCD peak and trough. This asymmetry continues to grow at longer times such that the trough nearly vanishes by 500 μs, long before CO recombination to T state Hb has had an opportunity to cancel the remaining ΔCD peak. These effects can be attributed mainly to the large R − T CD difference spectrum (Perutz et al., 1974a). The Soret CD of the T form is blue shifted and roughly double that of R so that R → T conversion gives both the peak and trough of the ΔCD a shift to more positive ellipticity.

A more quantitative estimate of the effect of the R − T difference in the time-resolved CD and absorption spectra can be given using the ca. 200-μs time constant for R + CO recombination (accompanying paper). About 8% of photolyzed heme recombines with CO within 15 μs, leaving the additional 5% drop in bleaching and the 4% shortfall in deoxy ΔOD peak decay attributed to the R − T absorption difference. In the same manner, we estimate for the CD a roughly 30% enhancement in loss of negative ellipticity at the trough and a 15% shortfall in deoxy decay due to the R → T difference. The much larger effect of R → T in the CD is in line with the much larger relative difference between deoxy R and T CD maximum intensities: $(T_{max} - R_{max})/R_{max}$ is five times larger in CD than in OD (Perutz et al., 1974a).

The CD measured at 500 μs, the last time probed in this TRCD study, roughly resembles that of the parent HbCO species in shape and size (Figure 3), although it is clear from the remaining red-shifted shoulder that the sample has not completely rebound all of the photolyzed CO. The transient species probed at this time corresponds mostly to a mixture of R state HbCO and T state deoxyHb, since nearly all deoxyhemes in the R quaternary state will have disappeared by either CO rebinding or R to T switching (Hofrichter et al., 1983, 1985; Murray et al., 1988). Note that both the ΔOD and ΔCD spectra in the Soret region are increasingly shifted to shorter wavelengths with time. This is most clear for the 500-μs ΔCD spectrum in Figure 4, where the isosbestic point (zero-crossing) is blue shifted by several nanometers from the early-time isosbestics. It has been proposed that a blue shift in the Soret bands is correlated with increasing distance of the iron out of the heme plane (Perutz et al., 1974c; Murray et al., 1988).

DISCUSSION

The most striking feature found in the near-UV TRCD of photodissociated HbCO is the prompt appearance of a negative ellipticity in the aromatic bands near 285 nm. This feature, assigned by Perutz et al. (1974a) to aromatic residues at the inter-dimer interfaces (Trp β37 and Tyr α42), is seen in static CD spectra only when the protein is in the T quaternary form. Its appearance in the TRCD of photolyzed Hb is strong evidence for a rapid shift of the $\alpha_1\beta_2$ interface to a more T-like conformation, with a time constant of approximately 500 ns. This shift precedes formation of the T state species that is found to appear in time-resolved absorption and resonance Raman with a 20 μs observed time constant, commonly taken as the time constant for the R → T transition. Jones et al. (1992) examined the dependence of HbCO relaxation kinetics on extent of photolysis and found that the 20-μs time constant slows with decreasing photolysis level, consistent with the expected decrease in R → T rate constant with increased ligation, whereas kinetics observed for relaxations on faster time scales appear insensitive to photolysis level. Thus, although the present study examines HbCO only under high photolysis conditions, the extent of photolysis is not expected to affect the kinetics of the sub-microsecond CD changes reported here.

The assignment of a T-like character to the nanosecond UV-TRCD transient is based on the appearance of negative ellipticity bands near 285 nm, considered the most distinctive spectral characteristic of the T quaternary state in static CD studies. This feature is present in equilibrium T state deoxyHb, absent in R state liganded Hb, and independent of heme ligation in the sense that hemoglobins modified to remain R state in the absence of ligands, through replacement or chemical modification of key residues, only show this CD feature when treated with allosteric effectors that induce the T quaternary state (Perutz et al., 1974a,b). Several aromatic absorption peaks lie within this band, with tryptophan and tyrosine being the strong absorbers (phenylalanine absorptions can be neglected as these are more than an order of magnitude weaker and lie to shorter wavelengths). Peaks at 294 and 302 nm in the R − T absorption difference, assigned to Trp β37(C3), vanish when this tryptophan is replaced by serine (Perutz et al., 1974b). R − T absorption peaks at 279 and 287 nm are assigned to tyrosine, probably Tyr α42(C7) since other candidates either have unchanged R and T environments or can be removed without affecting these peaks (Perutz et al., 1974a). Both Trp β37 and Tyr α42 are at the $\alpha_1\beta_2$ interface, where they experience large changes during the R → T transition. Relative motion of the dimers on going from the R to the T quaternary structure brings Trp $\beta_2$37 into close packing against Arg $\alpha_1$141(HC3) in the α_1FG/β_2C flexible joint region and into contact with the ring of Tyr $\alpha_1$140(HC2) at the carboxy terminus of the α_1 C helix. Tyr $\alpha_1$42 loosens contact with the guanidinium group of Arg $\beta_2$40(C6) and picks up a hydrogen bond to

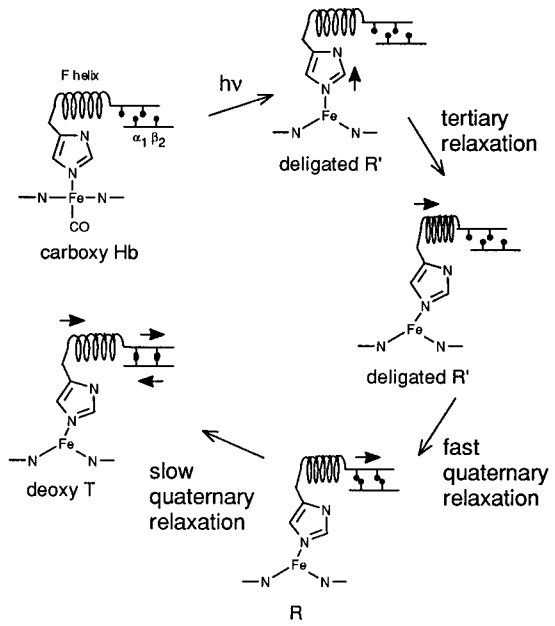

FIGURE 5: Scenario for compound R → T quaternary transition in photolyzed Hb-CO. Immediately after photodissociation, protein conformation is unrelaxed from the carboxyHb structure. This structure, designated R′, undergoes tertiary relaxation (100 ns) before a fast (1 μs) interfacial relaxation produces an intermediate quaternary structure, R [see also Goldbeck et al. (1996)]. The T state is reached from R after the 30-μs quaternary relaxation comprising dimer−dimer rotation and translation.

Asp $\beta_2$99(G1) at the α_1C/β_2FG switch region (Perutz & Fermi, 1981). Thus linked to changes in the environment of the aromatic residues in the $\alpha_1\beta_2$ interface, we take changes in the aromatic ellipticity near 285 nm as providing a robust diagnostic for the R → T quaternary structure transition (Perutz et al., 1974a,b).

The sequential appearance of spectrally distinct forms of T, or at least T-like, Hb leads to the inference of a stepwise mechanism for the R → T transformation. Given that the initial T-like form is a kinetic intermediate between the R and final T conformations, the questions then become what is the structural difference between the intermediate and final T forms and what does this imply for the overall mechanism of the R → T process? The implications of the TRCD results presented here, considered with the TROD results (Goldbeck et al., 1996), for the propagation of structural changes in Hb after photodissociation are discussed in terms of the allosteric core mechanism (Gelin & Karplus, 1977; Gelin et al., 1983). Within the allosteric core, composed of the heme, proximal histidine, part of the F helix, and the FG corner, structural changes at localized regions of the protein are coupled to structural changes at the heme associated with deligation. In particular, the F helix provides a conduit for the communication of mechanical forces between the proximal histidine−heme locus and the $\alpha_1\beta_2$ interface.

Our time-resolved spectral results are consistent with the following scenario for dynamics within the allosteric core leading to quaternary structure change, illustrated schematically in Figure 5. Doming of the heme after ligand photodissociation moves the iron out of the heme plane by as much as 0.5 Å (Fermi, 1975; Perutz et al., 1982). Some of this motion appears as a prompt (sub-picosecond) component, with the remainder appearing with a time constant of approximately 100 ns, as indicated by time-resolved resonance Raman studies of heme core-size frequencies (Terner et al., 1981; Stein et al., 1982; Spiro et al., 1990) and as is consistent with the ca. 100-ns time constant seen in the Soret and near-UV absorption spectra in the accompanying paper. The out-of-plane movement of the iron atom reduces steric forces between the proximal histidine and the pyrrole nitrogens operating to keep the histidine−heme bond angle perpendicular (tertiary relaxation within R′, Figure 5). This relaxation in tension associated with the histidine−heme bond angle is transmitted via the F helix conduit to the $\alpha_1\beta_2$ interface (Friedman, 1985; Findsen et al., 1985), triggering a rearrangement of protein conformation there that we associate with the early negative ellipticity observed in the aromatic TRCD and with the 1-μs relaxation observed in the TROD (fast quaternary relaxation, R′ → R). These changes at the $\alpha_1\beta_2$ interface probably correspond to breaking and reforming of H-bonds and nonbonded interactions between subunits, eventually leading to the relative rotation and translation of $\alpha_1\beta_1$ and $\alpha_2\beta_2$ dimers marking the R → T transition (slow quaternary relaxation). The nature of these changes is inferred from the observation at early probe times of large CD changes near 290 nm that are characteristic of a T state environment for aromatic residues at the $\alpha_1\beta_2$ interface (Perutz et al., 1974a,b).

The shift in protein conformation at the interface to more T-like character, at least near the aromatic residues, is reasonably associated with a greater pull by the F helix on the proximal histidine to produce further tilting of the histidine−heme bond angle. A concomitant perturbation of heme electronic structure would then underlie the 1-μs relaxation observed in the porphyrin absorption bands in the deligated hemes. Finally, the 20−30-μs TROD changes found to accompany completion of the R → T transition are attributed to further histidine tilt leading to the equilibrium deoxy heme position. Overall, the tilting of the histidine−Fe bond is found from resonance Raman experiments (Rousseau & Friedman, 1988) to evolve in a process composed of several relaxations that are in good agreement with the time constant found from TROD. The first relaxation, proceeding in conjunction with the out-of-plane displacement of Fe, produces 25% of total bond angle relaxation within 300 ns of photolysis, additional histidine relaxation occurs by about 1 μs (Rousseau & Friedman, 1988; Spiro et al., 1990), and the fully relaxed T state deoxy heme position is reached after a final 20 μs relaxation (Rousseau & Friedman, 1988).

The prompt appearance of T character in the aromatic TRCD, assigned to R′ → R, precedes the appearance of T character in the Soret region TRCD, the kinetics of the latter paralleling the 20−30-μs rate process assigned to the R → T transition in TROD studies. The inference of sequential structural changes in the protein from these observations rests on two factors: (1) empirical correlations with the equilibrium CD of R and T state Hb and (2) the assumption that the ΔCD signals are mostly due to changes in the CD-inducing dipole−dipole electronic interactions as protein residues and heme chromophores move relative to one another during tertiary and quaternary structural transitions. In this regard, the ΔCD associated with the aromatic bands probably reflects a more localized picture of protein structure changes (centered near the interface) than does the ΔCD in the Soret region, given the smaller transition strengths of the former. The contribution of heme-residue couplings, which could provide an exception to this consideration, has

been calculated by Hsu and Woody (1971) and found not to be well correlated to the CD of the aromatic residues. Hsu and Woody find, in particular, that the proximal histidine does not affect the Soret rotational strength significantly, so one would not expect the very local effect of this tilt to give rise to the large Soret deoxy heme CD changes seen on the microsecond time scale. The distal histidine is found, however, to contribute significantly to the Soret rotational strength, and, since distal perturbations have been suggested to contribute to heme−heme interactions (Levy et al., 1992), it is conceivable that distal changes occur on this time scale. Other factors that may contribute to the Soret ΔCD include acquisition of intrinsic heme chirality through distortion of the heme chromophore from nominal D_{4h} symmetry (Blauer et al., 1993) and heme−heme excitonic interactions (Woody, 1985), which may be expected to change during quaternary structural changes. Of the aromatic amino acids calculated by Hsu and Woody to contribute to the Soret rotational strength (1971), residues giving intra-subunit heme-residue couplings include Tyr α42(C7), Tyr α140(HC2), and Phe β41(C7), all at the $\alpha_1\beta_2$ interface, and Phe α43(CD1) and Phe β42(CD1), which are packed against their respective hemes. Inter-subunit couplings expected to contribute to the ΔCD include the coupling of heme α_1 with Trp $\beta_2$37 and Phe $\beta_2$41 and heme β_1 with Tyr $\alpha_2$42. The calculated contributions of inter-subunit heme-residue couplings and the suggestion by Woody (1985) that the high dipole strength of the Soret transition may give rise to significant heme−heme electronic interaction both support the idea that the Soret region ΔCD can reflect changes in the relative geometry of the $\alpha\beta$ dimers.

Although the negative ellipticity feature in the near UV region is strongly correlated with the T state in equilibrium CD studies, this is not inconsistent with its appearance prior to completion of the full R → T transition in the present time-resolved CD results. Apparently, the negative CD feature is first acquired through conformational changes at the interface during the R′ → R step along the kinetic pathway to the T state, as resolved by TRCD, but the obligatory decay of metastable R to T prevents the buildup of a significant population of the negative ellipticity R form in equilibrium studies and leaves the T state as the only observable equilibrium species carrying this CD marker.

The proposal that a metastable R conformation lies intermediate between the equilibrium R and T structures, and that this intermediate shows spectral perturbation of the interfacial aromatic residues before the full R → T transformation, finds additional support in recent X-ray results for a Y (Smith et al., 1991; Smith & Simmons, 1994) or R2 (Silva et al., 1992) oxyHb structure that is distinct from the classic R crystal structure. On the basis of crystallographic difference maps, Srinivasan and Rose (1994) suggest that the classic R structure is actually an intermediate along the pathway R2/Y → R → T [a pathway which we speculate may correspond to the sequence of kinetic species R′ → R → T inferred from TROD results (Goldbeck et al., 1996) and the present TRCD work]. Calculations of CD in the aromatic region are not available for hemoglobin, but it is reasonable to assume that a major contribution to the CD of Trp β37 comes from its interaction with Tyr α140, as these residues come into contact in the T state. Interfacial contacts calculated by Srinivasan and Rose (1994, Table 5) indicate that the Trpβ37−Tyrα42 interaction is already fully developed during the R2/Y → R step, suggesting that T state-like aromatic CD can be associated with the intermediate R X-ray structure. The crystallographic analysis thus parallels our proposal that T state-like aromatic CD appears with the metastable R intermediate.

Our interpretation of the early CD changes in the UV spectral region finds support in the growing evidence for early changes at the $\alpha_1\beta_2$ interface obtained from time-resolved UV resonance Raman studies. Su et al. (1989) found changes for the W3 band of Trp at the $\alpha_1\beta_2$ interface as early as 5 μs and peaking at 10 μs after photolysis, suggesting that the R → T transition occurs in a stepwise fashion with the formation and decay of a 10-μs intermediate. A similar study by Kaminaka et al. (1990) found protein structural changes evident by 10 μs after photolysis and left open the possibility that changes occur even earlier at the interface. Rodgers et al. (1992), repeating the work of Su et al. (1989), found that the R − T difference for Tyr α42 grew in monotonically with the same 10−20-μs time constant seen in the earlier work, as now did the W3 band for Trp β37. They further found a difference signal for the Trp β37 W17 band appearing at about 1 μs that later shifted in frequency to that seen in the static R − T difference, behavior that they suggested may reflect the sequential breaking and forming of intra-subunit hydrogen bonds to Trp β37 during a stepwise R → T transition. Most recently, Jayaraman et al. (1995) present resonance Raman evidence for the early appearance of T-like character at the interface. Moreover, they interpret the appearance of UV resonance Raman features marking the formation of T state hydrogen bonds for Trp β37 and Tyr α41 with a 0.5 μs time constant after HbCO photolysis as evidence for rotation of the dimers to their T state quaternary conformation before the 20-μs process usually identified as the R → T transition. The UV resonance Raman results thus parallel the UV TRCD results in finding the initial appearance of a T state-like environment at the interfacial aromatic residues by about 1 μs after photolysis. However, the hypothesis advanced by Jayaraman et al. (1995) to explain the UV resonance Raman results, in which they propose that the ca. 1-μs process corresponds to full rotation of the dimers to the T quaternary conformation and that the ca. 20-μs process simply reflects tertiary relaxation at the hemes, appears to be inconsistent with the results of absorption studies conducted at different photolysis levels. Jones et al. (1992) found that the rate constant of the 1-μs process is independent of the extent of photolysis, whereas the rate constant for the ca. 20-μs process slows with decreasing photolysis level. The dependence on ligation state inferred from this photolysis level study suggests that it is the slow relaxation that proceeds through the more cooperative reaction pathway rather than the opposite scenario proposed by Jayaraman et al. (1995).

To summarize our conclusions, time-resolved CD measurements on photolyzed HbCO reveal the sequential appearance of T-like character in separate spectral regions, with the near-UV CD of aromatic residues at the $\alpha_1\beta_2$ interface registering an early change at about 1 μs, followed by the appearance of T state CD in the Soret region with the 20−30-μs R → T time constant observed in the time-resolved absorption. The aromatic CD is expected to reflect the configuration of the protein environment more local to the interfacial aromatic residues, whereas the Soret CD reflects wider aspects of protein structure, including the quaternary

arrangement of Hb subunits. The sequential evolution observed in the TRCD spectra is therefore interpreted in terms of a compound R → T transition beginning with a conformational relaxation localized to residues at the $\alpha_1\beta_2$ interface, followed by the slower relaxation of global protein structure to the equilibrium T form. The fast process is considered here to be quaternary in the sense that it appears to alter subunit interactions, but the relative rotation and translation of dimer subunits that is usually associated with the term quaternary transition in hemoglobin occurs during the slow process. In the accompanying paper, the scenario for a compound R → T transition presented qualitatively here is cast into a microscopic kinetic model for HbCO photolysis and compared quantitatively to multichannel time-resolved UV−vis absorption data. The unpolarized absorption data have the advantage of a high signal-to-noise ratio for such a comparison, although being dominated by heme-based transitions they are less directly sensitive to quaternary structure than are the CD spectra. From the kinetic modeling in the accompanying paper we are able to identify more subtle spectrokinetic features in the Soret absorption band that correlate with the quaternary evolution observed in the UV−vis TRCD.

This study demonstrates some of the advantages and limitations of fast TRCD spectroscopy as a tool for probing conformational changes in proteins away from equilibrium. Relaxations in protein structure are made much more evident in TRCD spectra than in the corresponding absorption spectra by the exquisite sensitivity of CD to protein conformation. After photodissociation of HbCO, time evolution in the absorption spectrum can be accounted for almost entirely by heme ligation state changes, whereas the much larger R − T difference found in CD injects a correspondingly greater amount of structural information into the time evolution of the CD spectra. Assignment of the difference CD to particular structural changes has been aided by empirical comparisons with the static spectra of equilibrium structures and, in the Soret region, by the availability of spectral calculations for hemoglobin. The well-studied spectral properties of equilibrium Hb forms were applied in the present work to the characterization of nonequilibrium photolysis products, such as R_0. Although this procedure allowed the assignment of specific structural changes, such as the appearance of T-like character at the interface, on the basis of spectral similarities between equilibrium and photolysis difference spectra, the usual caveats about such extrapolations must be kept in mind, including the possibility that a conformational change particular to a metastable intermediate coincidentally introduces a spectral feature that has been assigned to an equilibrium structure. In this regard, we are currently investigating complementary spectroscopic approaches for obtaining information about conformational changes at the $\alpha_1\beta_2$ interface. In particular, the time-resolved magnetic circular dichroism of the aromatic residues offers an additional route to information about conformational relaxations affecting the interfacial tryptophans and tyrosines that may shed further light on the compound nature of the R → T process.

ACKNOWLEDGMENT

We thank Dr. Jim Lewis for invaluable technical assistance.

REFERENCES

Baldwin, J. M., & Chothea, C. (1979) *J. Mol. Biol. 129*, 175−220.
Björling, S. C., Goldbeck, R. A., Milder, S. J., Randall, C. E., Lewis, J. W., & Kliger, D. S. (1991) *J. Phys. Chem. 95*, 4685−4694.
Björling, S. C., Zhang, C.-F., Farrens, D. L., Song, P.-S., & Kliger, D. S. (1992) *J. Am. Chem. Soc. 114*, 4581−4588.
Blauer, G., Sreerama, N., & Woody, R. W. (1993) *Biochemistry 32*, 6674−6679.
Chen, E. F., Parker, W., Lewis, J. W., Song, P. S., & Kliger, D. S. (1993) *J. Am. Chem. Soc. 115*, 9854−9855.
Einterz, C. M., Lewis, J. W., Milder, S. J., & Kliger, D. S. (1985) *J. Phys. Chem. 89*, 3845−3853.
Fermi, G. (1975) *J. Mol. Biol. 97*, 237−256.
Findsen, E. W., Friedman, J. M., Ondrias, M. R., & Simon, S. R. (1985) *Science 229*, 661.
Friedman, J. M. (1985) *Science 228*, 1273.
Gelin, B. R., & Karplus, M. (1977) *Proc. Natl. Acad. Sci. U.S.A. 74*, 801.
Gelin, B. R., Lee, W.-M., & Karplus, M. (1983) *J. Mol. Biol. 171*, 489.
Geraci, G., Parkhurst, L. J., & Gibson, Q. H. (1969) *J. Biol. Chem. 244*, 4664.
Goldbeck, R. A., & Kliger, D. S. (1993) *Methods Enzymol. 226*, 147−177.
Goldbeck, R. A., Paquette, S. J., Björling, S. C., & Kliger, D. S. (1996) *Biochemistry 35*, 8628−8639.
Hofrichter, J., Sommer, J. H., Henry, E. R., & Eaton, W. A. (1983) *Proc. Natl. Acad. Sci. U.S.A. 80*, 2235.
Hofrichter, J., Henry, E. R., Sommer, J. H., Deutsch, R., Ikeda-Saito, M., Yonetani, T., & Eaton, W. A. (1985) *Biochemistry 24*, 2667.
Hsu, M.-C., & Woody, R. W. (1971) *J. Am. Chem. Soc. 93*, 3515.
Jackson, T. A., Lim, M., & Anfinrud, P. A. (1994) *Chem. Phys. 180*, 131−140.
Jayaraman, V., Rodgers, K. R., Mukerji, I., & Spiro, T. G. (1995) *Science 269*, 1843−1848.
Jones, C. M., Ansari, A., Henry, E. R., Christoph, G. W., Hofrichter, J., & Eaton, W. A. (1992) *Biochemistry 31*, 6692−6702.
Kaminaka, S., Ogura, T., & Kitagawa, T. (1990) *J. Am. Chem. Soc. 112*, 23.
Levy, A., Sharma, V. S., Zhang, L., & Rifkind, J. M. (1992) *Biophys. J. 61*, 750−755.
Lewis, J. W., Tilton, R. F., Einterz, C. M., Milder, S. J., Kuntz, I. D., & Kliger, D. S. (1985) *J. Phys. Chem. 89*, 289−294.
Murray, L. P., Hofrichter, J., Henry, E. R., & Eaton, W. A. (1988) *Biophys. Chem. 29*, 63.
Perutz, M. F. (1970) *Nature 228*, 726.
Perutz, M. F. (1972) *Nature 227*, 495.
Perutz, M. F. (1979) *Annu. Rev. Biochem. 48*, 327.
Perutz, M. F., & Fermi, G. (1981) *Hemoglobin and Myoglobin, Atlas of Molecular Structures in Biology*, Vol. 2, Oxford University Press, New York.
Perutz, M. F., Rossmann, M. G., Cullis, A. F., Muirhead, H., Will, G., & North, A. C. T. (1960) *Nature 185*, 416.
Perutz, M. F., Ladner, J. E., Simon, S. R., & Ho, C. (1974a) *Biochemistry 13*, 2163.
Perutz, M. F., Fersht, A. R., Simon, S. R., & Roberts, G. C. K. (1974b) *Biochemistry 13*, 2174.
Perutz, M. F., Heidner, E. J., Ladner, J. E., Beetlestone, J. G., Ho, C., & Slade, E. F. (1974c) *Biochemistry 13*, 2187.
Perutz, M. F., Hasnain, S. S., Duke, P. J., Sessler, J. L., Hahn, J. E. (1982) *Nature 295*, 535−538.
Perutz, M. F., Fermi, G., Luisi, B., Shannan, B., & Liddington, R. C. (1987) *Acc. Chem. Res. 20*, 309.
Petrich, J. W., Martin, J. L., Houde, D., Poyart, C., & Orszag, A. (1987) *Biochemistry 26*, 7914−7923.
Petrich, J. W., Poyart, C., & Martin, J. L. (1988) *Biochemistry 27*, 4049−4060.
Rodgers, K. R., Su, C., Subramaniam, S., & Spiro, T. G. (1992) *J. Am. Chem. Soc. 114*, 3697.
Rousseau, D. L., & Friedman, J. M. (1988) in *Biological Applications of Raman Spectroscopy, Vol. 3, Resonance Raman Spectra of Heme and Metalloproteins* (Spiro, T. G., Ed.) pp 133−215, Wiley, New York.

Savitzky, A., & Golay, M. J. E. (1964) *Anal. Chem. 36*, 1627.
Shapiro, D. B., Goldbeck, R. A., Che, D., Esquerra, R. M., Paquette, S. J., & Kliger, D. S. (1995) *Biophys. J. 68*, 326−334.
Silva, M. M., Rogers, P. H., & Arnone, A. (1992) *J. Biol. Chem. 267*, 17248−17256.
Smith, F. R., & Simmons, K. C. (1994) *Proteins 18*, 295−300.
Smith, F. R., Lattman, E. E., & Carter, C. W. (1991) *Proteins 10*, 81−91.
Spiro, T. G., Smulevich, G., & Su, C. (1990) *Biochemistry 29*, 4497−4508.
Srinivasan, R., & Rose, G. D. (1994) *Proc. Natl. Acad. Sci. U.S.A. 91*, 11113−11117.
Stein, P., Terner, J., & Spiro, T. G. (1982) *J. Phys. Chem. 86*, 168.
Su, C., Park, Y. D., Liu, G.-Y., & Spiro, T. G. (1989) *J. Am. Chem. Soc. 111*, 3457.
Terner, J., Stong, J. D., Spiro, T. G., Nagumo, M., Nicol, M., & El-Sayed, M. A. (1981) *Proc. Natl. Acad. Sci. U.S.A. 78*, 1313.
Waleh, A., & Loew, G. H. (1982) *J. Am. Chem. Soc. 104*, 2346.
Woody, R. W. (1985) in *Optical Properties and Structure of Tetrapyrroles* (Blauer, G., & Sund, H., Eds.) pp 239−256, Walter de Gruyter & Co., New York.

BI952247S